Inorg. Chem. **2003**, *42*, 7060–7066

The Structure of Magnesium Alanate

Maximilian Fichtner,*,† Jens Engel,† Olaf Fuhr,† Andreas Glöss,† Oliver Rubner,† and Reinhart Ahlrichs†,‡

Karlsruhe Research Center, Institute of Nanotechnology, POB 3640, D-76021 Karlsruhe, Germany, and University of Karlsruhe, Institute of Theoretical Chemistry, Fritz-Haber-Weg 4, D-76131 Karlsruhe, Germany

Received February 14, 2003

$Mg(AlH_4)_2$ was produced as a nanocrystalline powder by metathesis of $NaAlH_4$ and $MgCl_2$. Starting with a structure estimation which was developed from an evaluation of FTIR data and comparison of structural properties of two solvent adducts, quantum chemical calculations were performed on the density functional theory (DFT) level. The calculated atomic positions were used to simulate an X-ray powder diffraction pattern, based on a trigonal unit cell. The simulated pattern was congruent to experimental data. Thus, magnesium alanate exhibits a CdI_2 layer structure, the layers being formed by Mg atoms occupying the Cd sites and AlH_4 tedrahedra occupying the sites of the iodine atoms in CdI_2.

1. Introduction

Alkali tetrahydroaluminates, known as useful hydrogenating reagents in syntheses, were studied extensively in the past.[1−3] However, little is known about the earth alkaline compounds. Among these, $Mg(AlH_4)_2$ was first synthesized by Wiberg and Bauer[4,5] by the following routes:

$$4MgH_2 + 2AlCl_3 \rightarrow Mg(AlH_4)_2 + 3MgCl_2 \quad (1)$$

$$MgH_2 + 2AlH_3 \rightarrow Mg(AlH_4)_2 \quad (2)$$

$$2LiAlH_4 + MgBr_2 \rightarrow Mg(AlH_4)_2 + 2LiBr \quad (3)$$

The reactions were carried out in diethyl ether under inert conditions, yielding a white solid which was thermally stable up to 140 °C. The structure of magnesium alanate has been unknown prior to the work presented here.

In the past, Ashby and co-workers reported about the formation of $Mg(AlH_4)_2$ in THF solution[6] and characterized the bis and tetrakis solvent adduct by IR spectroscopy and X-ray powder diffractometry. Noeth et al.[7] produced single crystals from the tetrakis adduct $Mg(AlH_4)_2 \cdot 4THF$ and determined the structure by X-ray diffraction. Recently, the structure of the diethyl ether adduct $Mg(AlH_4)_2 \cdot Et_2O$ was determined by evaluating X-ray diffraction data obtained from single crystals.[8] In the same work, the structure of the tetrakis THF adduct proposed by Noeth et al. was confirmed.

No sufficiently large single crystals are obtained for structure determination by X-ray diffraction as the pure $Mg(AlH_4)_2$ forms an ultrafine, nanocrystalline powder after desolvation of the adduct.[8] To determine the structure of $Mg(AlH_4)_2$, our first approach was to interpret FTIR and X-ray diffraction data of the solvent adducts and the FTIR data of the pure alanate, leading to a first guess for the structure. Molecular electronic structure calculations were performed for clusters of $MgAl_2H_8$ units using density functional theory in order to develop a model of the crystal structure.

Therefore, the most stable cluster geometries were systematically investigated and extrapolated to the solid. This survey led us to a layered, CdI_2-like structure for $MgAl_2H_8$.

The calculated atomic positions were verified by comparison of a simulated XRD pattern with experimental XRD data by a Rietveld refinement. The computational details of this approach to obtain crystal structures from first principles calculations will be covered in a forthcoming paper.

* Corresponding author. E-mail address: fichtner@int.fzk.de. Phone: +49-7247 82 5340. Fax: +49-7247 82 6368.
† Karlsruhe Research Center, Institute of Nanotechnology.
‡ University of Karlsruhe, Institute of Theoretical Chemistry.

(1) Finholt, A. E.; Bond, A. C.; Schlesinger, H. I. *J. Am. Chem. Soc.* **1947**, *69*, 1199.
(2) Mikheeva, V. I.; Selivokhina, M. S.; Kryukova, O. N. *Dokl. Akad. Nauk SSSR* **1956**, *109*, 487.
(3) Mukhidinov, J. *Izv. Akad. Nauk.* **1993**, *1*, 29.
(4) Wiberg, E.; Bauer, R. *Z. Naturforsch.* **1950**, *5b*, 397.
(5) Wiberg, E.; Bauer, R. *Z. Naturforsch.* **1952**, *7b*, 131.
(6) Ashby, E. C.; Schwartz, R. D.; James, B. D. *Inorg. Chem.* **1970**, *9* (2), 325.
(7) Noeth, H.; Schmidt, M.; Treitl, A. *Chem. Ber.* **1995**, *128*, 999.
(8) Fichtner, M.; Fuhr, O. *J. Alloys Compd.* **2002**, *345*, 286.

10.1021/ic034160y CCC: $25.00
Published on Web 10/01/2003

2. Experimental Section

2.1. Synthesis. The solids were handled in an argon-filled glovebox equipped with a recirculation system to keep the water and oxygen concentrations below 1 ppm during operation. Synthesis was carried out on the bench under a vacuum or in inert gas (N_2) using Schlenk tube techniques.

Diethyl ether was distilled over sodium before use. Sodium alanate (purum, Sigma-Aldrich) was used in a 1 M THF solution as received. Solvent-free $NaAlH_4$ was obtained by drawing the THF off under a vacuum and heating the dry white solid to 50 °C until a residual pressure of 2×10^{-3} mbar was reached. Magnesium chloride (98%, Sigma-Aldrich) was used as received.

2.2. Instrumental Analysis. Solid-state infrared spectra of the alanates (as KBr pellets) were recorded in the range 5000−370 cm^{-1} under ambient conditions in air by using a Perkin-Elmer Spectrum GX FTIR spectrometer. No significant difference was observed between two subsequently taken spectra; effects caused by the ambient humidity were therefore excluded. The evaluation was done with the Perkin-Elmer Spectrum v. 2.00 Software.

The powder X-ray diffraction measurements were performed with a PHILIPS X'PERT diffractometer (Ni-filtered Cu Kα radiation, 2 kW, with X'Celerator RTMS detector, automatic divergence slit). The powder was wetted with mineral oil, and the slurry was spread and measured on an Si single crystal. For data acquisition and evaluation, the X'PERT 1.3e and ProFit 1.0c software were used.

3. Results

3.1. Synthesis of $Mg(AlH_4)_2$. Magnesium alanate was synthesized via a metathesis of sodium alanate and magnesium chloride. The synthesis procedure followed a proposition made by Wiberg and Bauer[4] and is described in detail elsewhere.[8]

$$2NaAlH_4 + MgCl_2 \rightarrow Mg(AlH_4)_2 \cdot Et_2O + 2NaCl \quad \text{in } Et_2O \tag{4}$$

$$Mg(AlH_4)_2 \cdot Et_2O \xrightarrow{\Delta} Mg(AlH_4)_2 + Et_2O\uparrow \tag{5}$$

The solvent adduct precipitated together with NaCl (eq 4) and was separated from the halide by Soxhlet extraction with diethyl ether. After removal of the ether, a white residue was obtained, which was dried at 90 °C in a vacuum to remove the solvent molecules in the ether adduct (eq 5). The final product was a fine white nanocrystalline powder.[8]

3.2. Instrumental Analysis. Elemental Analysis. According to elemental analysis, the product contained 9.02 ± 0.08 wt % H (theoretical: 9.34 wt %) and 2.3 ± 0.2 wt % C from residual organics. Residual amounts of 1.7 ± 0.1 wt % NaCl were detected in the product using the Mohr method. Thus, the purity was approximately 95%.

FTIR. The three solid-state IR spectra in Figure 1 were taken from the two solvent adducts and the pure $Mg(AlH_4)_2$. Signals at 2850−3050 and 1000−1200 cm^{-1} can be found only with the solvent adducts of $Mg(AlH_4)_2$ and are due to the C−H and C−O−C vibrational transitions of the bound solvent molecules, THF or diethyl ether. As can be seen in Figure 1a, the absorption is much stronger for the THF adduct in these bands, as there are four solvent molecules instead of only one in the diethyl ether adduct.

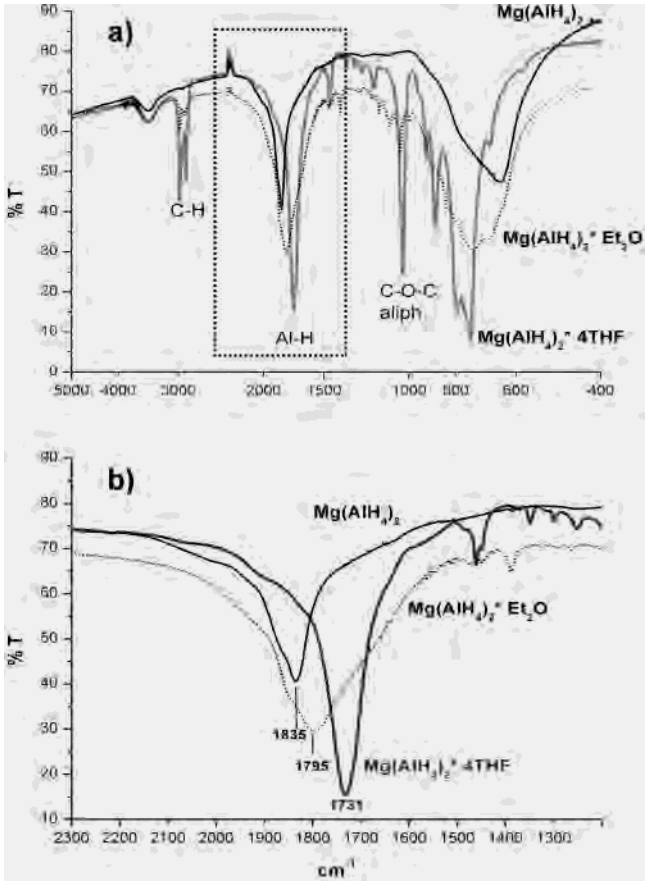

Figure 1. (a) Solid-state FTIR spectra of $Mg(AlH_4)_2$, $Mg(AlH_4)_2 \cdot 4THF$, and $Mg(AlH_4)_2 \cdot Et_2O$. (b) Region of the Al−H vibration (ν_3).

Table 1. Experimental Data Regarding Fundamental Frequencies (in cm^{-1}) of the AlH_4^- Ion[a]

	ν_1	ν_2	ν_3	ν_4
Al−H	1790	799	1740	764

[a] The ν_3 and ν_4 transitions are IR-active.[12]

According to Nakamoto,[12] the tetrahedral hydrides MH_4 and ions have four natural modes of vibrations, which are all Raman-active. Only the antisymmetric stretching modes ν_3 and ν_4 are infrared-active. Experimental data of the fundamental frequencies of the AlH_4^- ion are listed in Table 1. According to the table, vibrational transitions can be found in the region around 1600−2000 cm^{-1} (ν_3) and the fingerprint region (ν_4).

A closer look at the ν_3 band of the magnesium alanate and its solvent adducts reveals peak shoulders, indicating H-atoms in different binding states. When comparing the three Al−H bands, a shift of the peak values in the order of

$$\nu_{Al-H}(Mg(AlH_4)_2 \cdot 4THF) < \nu_{Al-H}(Mg(AlH_4)_2 \cdot Et_2O) < \nu_{Al-H}(Mg(AlH_4)_2)$$

is apparent from Figure 1b. The peak shift is assigned to an increasing covalent character of the Al−H bonds in the compounds. This may be due to an increasing number of H-atoms bridging Al and Mg in the THF adduct (2 bridging H-atoms per formula unit) and the diethyl ether adduct (5 bridging H-atoms), leading to stronger terminal Al−H bonds

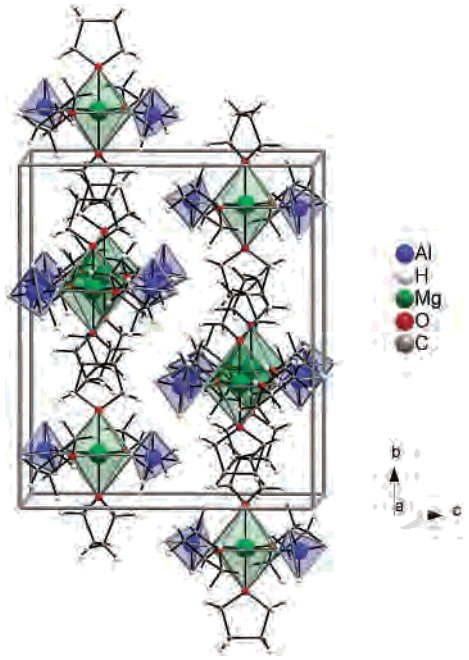

Figure 2. Crystal structure of $Mg(AlH_4)_2 \cdot 4THF$.[8]

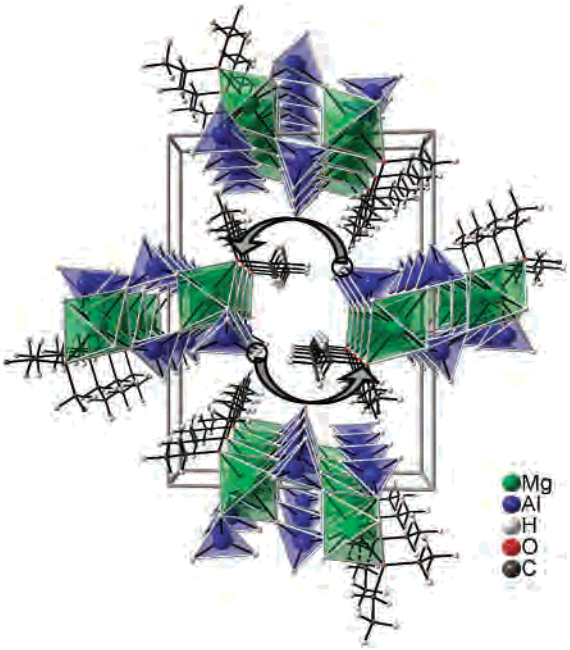

Figure 3. Crystal structure of $Mg(AlH_4)_2 \cdot Et_2O$.[8] The arrows indicate the proposed mechanism of transformation into $Mg(AlH_4)_2$ when the solvent is released and substituted by a terminal H-atom of a formerly $\mu 2$ bridging AlH_4 unit.

in the latter case. These interpretations are in accordance with the observations made by Ashby et al.[6]

Considering the peak shift, the solvent-free $Mg(AlH_4)_2$ seems to have even more H-bridges in its structure than the solvent adducts. We explained this peak shift with a reaction mechanism where the bond between Mg and the solvent molecule is released and the free octahedral coordination site is occupied by a terminal hydrogen atom of a formerly $\mu 2$ bridging AlH_4 tetrahedron (see arrows in Figure 3). This would result in a sheet structure of $Mg(AlH_4)_2$, consisting of MgH_6 octahedra which are linked by $\mu 3$ bridging AlH_4 tetrahedra.

X-ray Diffraction. X-ray diffraction patterns were taken of powder samples, the pattern indicating a structure of high symmetry. As the peaks were obviously broadened, an analysis of the peak shapes was performed, and the volume-weighted mean grain size from Bragg-peak broadening, corrected for strain, was determined.[13,14] The results indicated that the mean crystallite size was reduced to 30 ± 4 nm after the drying procedure, whereas the crystallite size of the ether adduct was much higher (approximately 3 μm).

3.3. Possible Mechanism of Solvent Release. The structures of $Mg(AlH_4)_2 \cdot 4THF$ and $Mg(AlH_4)_2 \cdot Et_2O$ have been determined by single-crystal X-ray diffraction.[8] Figures 2 and 3 show the respective molecular packings in the lattice.

The THF adduct consists of single molecules with a central magnesium atom that is octahedrally coordinated by two opposing AlH_4 tetrahedra and four THF molecules bound via the oxygen atoms. The diethyl ether adduct has the same constituents: AlH_4 tetrahedra and octahedrally coordinated magnesium. Here, the crystal is made up of double strands of Mg-octahedra which are interconnected at 5 positions via shared H-atoms by $\mu 2$ or $\mu 3$ bridging AlH_4 tetrahedra. The last free coordination site is saturated by the oxygen atom of an ether molecule, as shown in Figure 3.

According to the measured powder diffraction patterns, desolvation from the THF and the diethyl ether adduct lead to samples of solvent-free $Mg(AlH_4)_2$ having the same crystal structure.

This observation may be rationalized as follows. If the solvent is removed from the strands of the diethyl ether adduct, the free coordinative Mg sites can be connected with former $\mu 2$ bridging AlH_4 units to form sheets consisting of MgH_6 octahedra and AlH_4 tetrahedra, as shown in Figure 6.

The desolvation of the THF adduct may proceed via intermediates having an increasing number of bridging hydrogen atoms. This assumption is supported by the results of FTIR measurements, see section 3.2. We analyzed samples of the THF adduct at various stages of the drying procedures and found a continuous shift of the Al−H stretching vibration to higher wavenumbers until the end value of the desolvated magnesium alanate was reached. The existence of a possible intermediate, $Mg(AlH_4)_2 \cdot 2THF$, was reported by Ashby et al.[6] who also found indications for bridging hydrogen atoms in the infrared spectrum. An intermediate similar to the diethyl ether adduct can be obtained by removing one more THF molecule from each Mg octahedron leading to a double-strain structure, which would be fully equivalent to the ether adduct except for the ether being replaced by a THF molecule.

3.4. Calculation of the Structure. As it was not possible to grow single crystals for pure $Mg(AlH_4)_2$, the experimental verification of the crystal structure had to be based on powder diffraction data.

In our approach to determine the crystal structure and thermodynamic data of pure magnesium alanate, we performed extensive calculations for a variety of clusters that served as models of the bulk structure. We considered about 70 clusters of $(Mg(AlH_4)_2)_n$ of up to $n = 42$, which included strands and two-, and three-dimensional skeletons of the

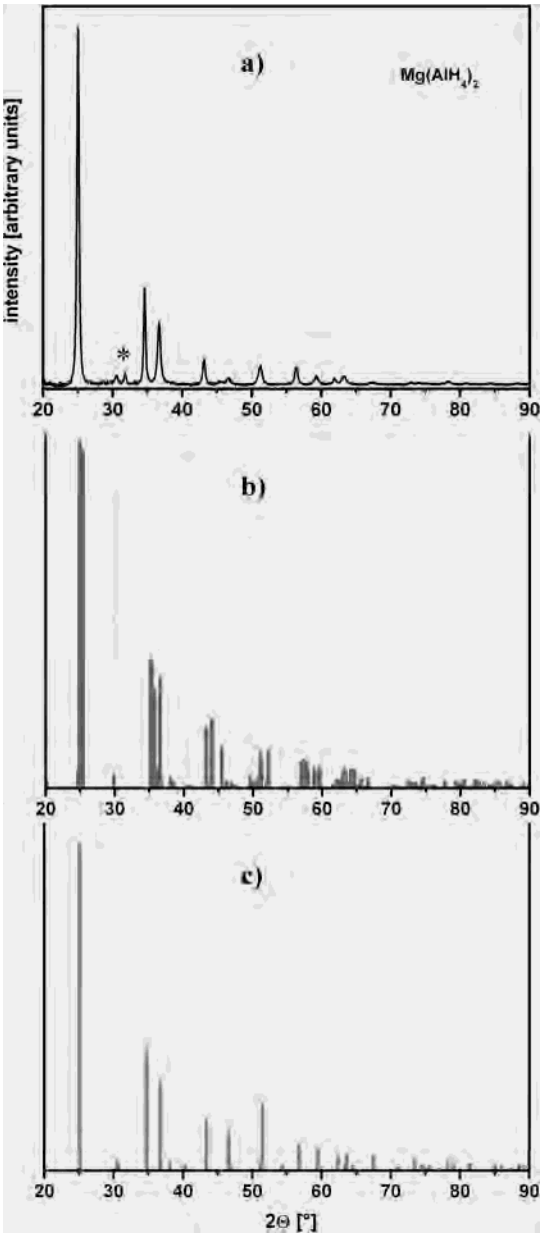

Figure 4. (a) Experimental XRD data of $Mg(AlH_4)_2$. The asterisk in the upper panel indicates the presence of an NaCl impurity in the sample. (b) Simulated XRD pattern of the computed triclinic structure of $Mg(AlH_4)_2$. (c) Simulated XRD pattern of the trigonal structure of $Mg(AlH_4)_2$.

heavy atoms Mg and Al. The quantum chemical calculations were carried out with the program package Turbomole on the RI-DFT level with a B-P86 functional.[9−11] Several tests in comparison with bigger basis sets (TZVP, TZVPP) have shown that a SV(P) basis set yields sufficiently accurate energies and geometries. Because of the size of the systems needed to perform a reasonable extrapolation to the solid, the less expensive DFT calculations were chosen. A detailed analysis of these calculations together with a discussion of the estimated errors will be published in a forthcoming paper.[25]

The most stable clusters obtained in this way were those with octahedrally coordinated Mg atoms and tetrahedrally coordinated Al atoms in a CdI_2-like sheet structure. To extrapolate the results to the solid, small and medium clusters of single, double, and triple layers were constructed and the cohesion energy per monomer was chosen as a measure for the reliability of the extrapolation. This fictitious quantity measures the energy gain when combining single $Mg(AlH_4)_2$ molecules in the gas phase to a solid (see section 3.5). The suitability of such an extrapolation scheme has been demonstrated earlier, e.g., on $MgCl_2$ and CdSe clusters.[23]

As surface effects in the calculated layers lead to a distorted geometry compared to an ideal crystal, it was not possible to extract a unit cell directly from the clusters. Therefore, we chose the innermost, least distorted part of a $(Mg(AlH_4)_2)_{30}$ double layer as a reference. This cut contained eight Mg atoms at the corners and two AlH_4 units inside.

In order to set up a unit cell for the crystal that can be periodically continued, it was necessary to shift the Mg atoms to obtain a parallelepiped. The shift was done so that the total squared deviation of the atomic coordinates from the initial structure was minimized. This led to a displacement of the atoms of 0.1 Å on the average, which is about 2% of the shortest cell constant. These shifts are still on the order of the well-known uncertainty of the DFT method itself.

As we imposed no symmetry constraints, the best-fit unit cell obtained this way was triclinic with the following cell parameters: $a = 5.099$ Å, $b = 5.088$ Å, $c = 5.978$ Å and $\alpha = 91.5°$, $\beta = 91.5°$, $\gamma = 120.2°$.

In Figure 4b, a simulated powder XRD pattern of the triclinic cell is compared to the experimental one in Figure 4a.

The calculated atomic positions and cell parameters show only slight deviations from those of a trigonal structure of the space group $P\bar{3}m1$. Hence, a Rietveld refinement of the

(9) Eichkorn, K.; Treutler, O.; Oehm, H.; Haeser, M.; Ahlrichs, R. *Chem. Phys. Lett.* **1995**, *242*, 652.
(10) Eichkorn, K.; Weigend, F.; Treutler, O.; Ahlrichs, R. *Theor. Chem. Acc.* **1997**, *97*, 119.
(11) Treutler, O.; Ahlrichs, R. *J. Chem. Phys.* **1995**, *102*, 346.
(12) Nakamoto, K. *Infrared Spectra of Inorganic and Coordination Compounds*, 2nd ed.; Wiley-Interscience: New York, 1979; p 108.
(13) Klug, H. P.; Alexander, L. E. *X-ray Diffraction Procedures for Polycrystalline and Amorphous Materials*; Wiley: New York, 1974; p 661.
(14) Krill, C. E.; Birringer, R. *Philos. Mag. A* **1998**, *77*, 621.
(15) Lundqvist, B. I.; Andersson, Y.; Shao, H.; Chan, S.; Langreth, D. C. *Int. J. Quantum Chem.* **1995**, *56*, 247.
(16) Kohn, W.; Meir, Y.; Makarov, D. E. *Phys. Rev. Lett.* **1998**, *80* (19), 4153.
(17) Lein, M.; Dobson, J. F.; Gross, E. K. U. *J. Comput. Chem.* **1999**, *20*, 12.
(18) Ahlrichs, R.; Elliot, S. D. *Phys. Chem. Chem. Phys.* **1999**, *1*, 13.
(19) Cox, J. D.; Wagman, D. D.; Medvedev, V. A. *CODATA Key Values for Thermodynamics*; Hemisphere Publishing Corp.: New York, 1989.
(20) Hauback, B. C.; Brinks, H. W.; Fjellvåg H. *J. Alloys Compd.* **2002**, *346*, 1−2, 184.
(21) Hauback, B. C.; Brinks, H. W.; Jensen, C. M.; Murphy, K.; Maeland, A. J. *J. Alloys Compd*., in press.
(22) Zachariasen, W. H.; Holley, C. E.; Stamper, J. F. *Acta Crystallogr.* **1963**, *16*, 352.
(23) Eichkorn, K.; Schneider U.; Ahlrichs, R. *J. Chem. Phys.* **1995**, *102*, 7557. Deglmann, P.; Ahlrichs, R.; Tsereteli, K. *J. Chem. Phys.* **2002**, *116*, 1585.
(24) Larson, A. C.; Von Dreele, R. B. *General Structure Analysis System (GSAS)*; Report LAUR 86-748; Los Alamos National Laboratory: Los Alamos, NM, 2000.
(25) Glöss, A.; Rubner, O.; Ahlrichs, R. Manuscript in preparation.

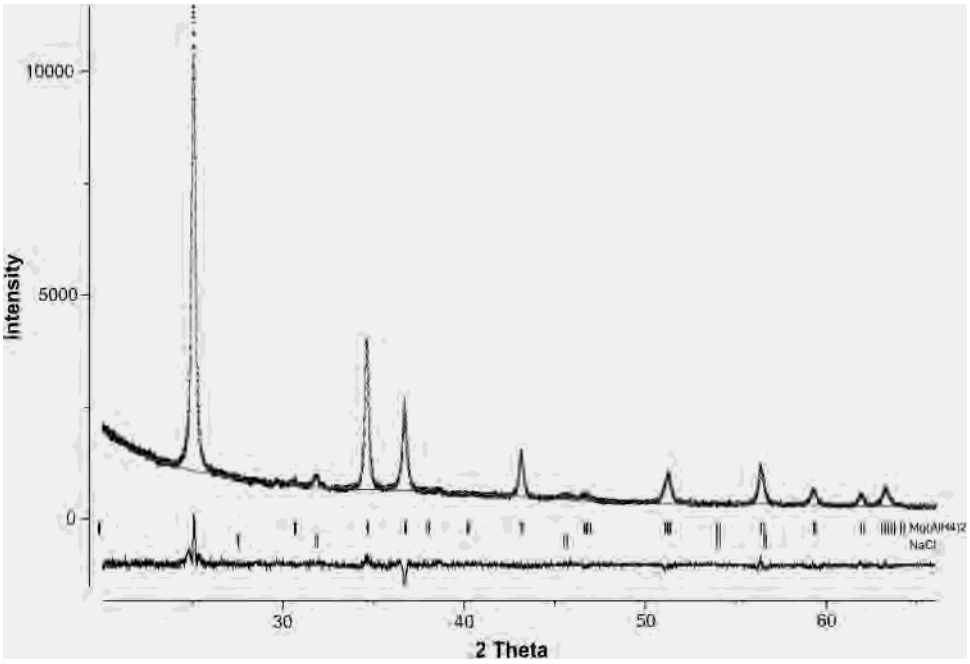

Figure 5. X-ray powder diffraction pattern of $Mg(AlH_4)_2$. Experimental data points are shown as dots; the refined simulated pattern and the background are shown as continuous lines. The small markers indicate the peak positions of $Mg(AlH_4)_2$ and NaCl. At the bottom is shown the differential spectrum $I_O - I_C$ of the observed and the simulated intensities.

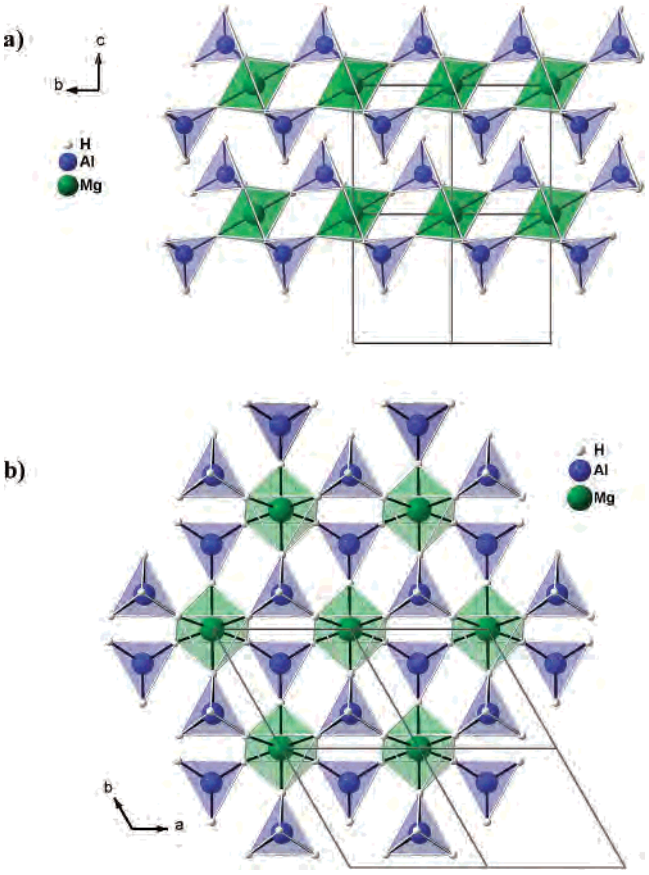

Figure 6. Trigonal structure of $Mg(AlH_4)_2$, space group $P\bar{3}m1$. (a) Double layer, view along the *a*-axis. (b) Single layer, view along the *c*-axis.

experimental pattern was done on the basis of this space group, in order to check the congruence with the experimental data. The 5509 data points were processed using *GSAS General Structure Analysis System*, version 2003, and the graphical interface *EXPGUI*.[24] The refinement technique used by GSAS is the method of least squares with the minimization function $M_P = \sum w(I_o - I_c)^2$.

Figure 5 shows an experimental pattern (I_o) and the simulated pattern from the Rietveld analysis (I_c). Below these are shown the reflection markers for $Mg(AlH_4)_2$ and NaCl, an impurity in the sample, and the difference pattern $I_o - I_c$. The diagram indicates that the peak positions fit well to the $P\bar{3}m1$ space group and the observed reflections can be explained completely by a superposition of the alanate and the NaCl pattern. The values of the residuals R_p and R_w were 0.0454 and 0.0609, and 13 parameters were used in the refinement procedure. The value for the goodness of fit (GOF $= R_w/R_{exp}$) was 1.68 (R_{exp}: expected R_w). R_p and R_w are defined as $R_p = \sum|I_o - I_c|/\sum I_o$ and $R_w = \sqrt{M_p/\sum w I_o^2}$.

According to the Rietveld analysis, the cell parameters of the trigonal cell are $a = b = 5.199$ Å, $c = 5.858$ Å and $\alpha = \beta = 90°$, $\gamma = 120°$. The calculated density of the $Mg(AlH_4)_2$ is 1.046 g/cm^3; the formula weight of the unit cell is 86.34. The atomic positions of the trigonal structure are given in Table 3. The Al atoms occupy the ($^1/_3$, $^2/_3$, z) and ($^2/_3$, $^1/_3$, $\bar{z}$) sites ($z = 0.7$; Wyckoff letter 2d)). However, a comparison of the XRD patterns can only give evidence for the positions of the metal atoms. For the hydrogen atoms bridging Mg and Al, we identified the positions closest to a 6-fold site (Wyckoff letter 6i (x, $\bar{x}$, z), $x = 0.16$, $z = 0.81$). The nonbridging hydrogen atoms were assigned to a 2-fold site (Wyckoff letter 2d ($^1/_3$, $^2/_3$, z), $z = 0.45$). These positions are given in Table 3; computed positions are given in Table 2. The mean deviations of the computed positions from the ideal ones were 0.35 Å (i) and 0.32 Å (d).

The bond lengths were calculated for the trigonal structure with the refined cell parameters and are 1.69 Å for the

Table 2. Computed Atomic Positions of $Mg(AlH_4)_2$

atom	*x*/*a*	*y*/*b*	*z*/*c*
Mg	0	0	0
Al1	0.33	0.64	0.71
Al2	0.66	0.34	0.30
H1	0.36	0.21	0.15
H2	0.58	0.35	0.55
H3	0.90	0.67	0.20
H4	0.08	0.31	0.81
H5	0.22	0.86	0.84
H6	0.3	0.66	0.45
H7	0.67	0.76	0.80
H8	0.82	0.12	0.24

[a] DFT results adapted to a triclinic unit cell with $a = 5.099$ Å, $b = 5.088$ Å, $c = 5.978$ Å, and $\alpha = 91.5°$, $\beta = 91.5°$, $\gamma = 120.2°$.

Table 3. Atomic Positions of $Mg(AlH_4)_2$ in the Trigonal Cell, Space Group $P\bar{3}m1$[a]

Mg (1a)	0	0	0
Al (2d)	$^1/_3$	$^2/_3$	0.7
H1 (2d)	$^1/_3$	$^2/_3$	0.45
H2 (6i)	0.16	-0.16	0.81

[a] H1 are non-bridging and H2 are bridging hydrogen atoms. The letters in parentheses are the corresponding Wyckoff letters. Unit cell parameters obtained from Rietveld refinement: $a = b = 5.199$ Å, $c = 5.858$ Å and $\alpha = \beta = 90°$, $\gamma = 120°$.

distances of Al to the bridging hydrogen atoms (H2) and 1.46 Å for the distance of Al to the nonbridging H atom (H1). The distances found in other alanates are between 1.603 and 1.63 Å in $LiAlD_4$[20] where the AlH_4 unit also forms a distorted tetrahedron, and 1.63 Å in $NaAlD_4$.[21] In AlH_3, the bond length is 1.715 Å.[26] Hence, in magnesium alanate the distances of the bridging H atoms to Al are close to those of AlH_3, while the length of the terminal Al−H bond is significantly shorter than any of the other Al−H bonds found in the compounds above. The bond length of Mg−H is 1.81 Å., which is smaller than in the binary hydride MgD_2 (1.95 Å).[22]

A representation of the trigonal structure of $Mg(AlH_4)_2$ is shown in Figure 6. It is equivalent to that of a CdI_2 sheet structure with Mg occupying the Cd sites and distorted AlH_4 tetrahedra occupying the iodine sites.

3.5. Calculation of Thermodynamic Properties. The cohesion energies per monomer of the calculated clusters $(Mg(AlH_4)_2)_n$ have been extrapolated to $n \rightarrow \infty$, as shown in Figure 7 for single layers. It is assumed that the surface and edges contributions to the total energy *E* depend on the number of $Mg(AlH_4)_2$ monomers within the layer as

$$E_n = E_\infty \cdot n + \alpha \cdot \sqrt{n} \qquad (6)$$

where the first term describes the plane contribution and the second term with some unknown coefficient α describes the contribution of the edges. Thus, a plot of the cohesion energy $\epsilon_n = E_n/n$ per monomer versus $1/\sqrt{n}$ should yield a straight line with an axis intercept of ϵ_∞, i.e., the cohesion energy per monomer of an infinite layer. Figure 7 shows that the results of the calculations are in excellent agreement with this assumption and the cohesion energy can be extracted as 148.9 kJ/mol.

(26) Turley, J. W.; Rinn, H. *Inorg. Chem.* **1969**, *8*, 18.

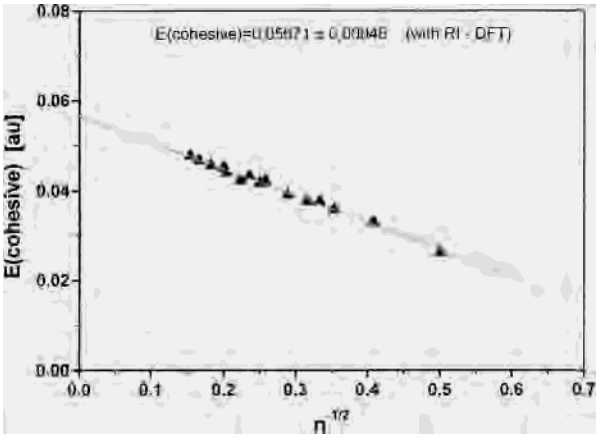

Figure 7. Linear fit of calculated cohesion energies ϵ_n per monomer for single $(Mg(AlH_4)_2)_n$ layers.

Due to the size of the clusters, we could only perform five calculations on 3-D clusters of reasonable size. The interactions between the layers are proportional to the size of the layers, and thus, they contribute a constant value to a plot of the energy over $1/\sqrt{n}$. For small clusters, this layer−layer interaction has been found to be 6.9 kJ/mol which leads to a total cohesion energy of 155.8 kJ/mol.

This value is corrected for the basis set superposition error (BSSE) arising when calculating stacked layers. Yet, it is well-known that DFT calculations often fail to describe the interactions of nonchemically bound layers.[15−17] This is also revealed by our calculations. We see that the layers tend to drift away from each other and reach an equilibrium distance which is too large (598 pm) compared with the distance obtained by XRD inspection (584 pm). Thus, the value for the layer−layer interaction can just provide an estimate.

Along with the calculations on $Mg(AlH_4)_2$, cluster models of solid MgH_2 have been computed. It was possible to determine the formation enthalpy of magnesium alanate and the reaction enthalpy of hydrogen desorption according to

$$Mg + 2Al + 4H_2 \rightarrow Mg(AlH_4)_2 \quad \Delta H_f \qquad (7)$$

$$Mg(AlH_4)_2(s) \rightarrow MgH_2(s) + 2Al(s) + 3H_2 \quad \Delta H_r \qquad (8)$$

The values for solid aluminum were taken from Ahlrichs,[18] while the standardized Mg atomization energy was used for the formation enthalpy.[19] The computed values are

$$\Delta H_f(Mg(AlH_4)_2(s)) = -64.8 \text{ kJ/mol}$$

$$\Delta H_r(\text{desorption}) = +41 \text{ kJ/mol}$$

In these values, zero point energies obtained for small clusters have been included as an approximation for the solid.

As we are currently not able to calculate the corrections of the given values, which result from temperature effects, the results are values for 0 K. We are aware of the fact that the calculated data should be treated as a first estimate only, due to the errors of the method itself and a certain deviation which results from the vibrational state of the crystal at 298 K.

4. Summary

In this work, we presented calculations on the crystal structure of magnesium alanate. From considerations of possible processes occurring during the loss of the solvent molecules by heating, a CdI_2-like layered structure was assumed. Extensive DFT calculations on different configurations were carried out. The energetically most favored structures were found to be equivalent to the CdI_2 framework. Clusters of those layers were investigated further, and an extrapolation to the solid was performed. A Rietveld refinement was performed, and near perfect agreement was found between a trigonal cell ($a = b = 5.199$ Å, $c = 5.858$ Å, $\alpha = \beta = 90°$, $\gamma = 120°$) of space group $P\bar{3}m1$ and the ab initio calculated atomic positions for the internal heavy atoms. To match the experimental XRD pattern, the computed atomic positions of the metal atoms had to be shifted by values which are on the order of DFT errors. If the hydrogen atoms are taken into account, the space group is retained. In the solid, the alanate sheets consist of octahedrally coordinated Mg atoms which are interconnected by AlH_4 tetrahedra. Three of the four hydrogen atoms of each tetrahedron serve as H bridges; one hydrogen is always terminally bonded perpendicular to the plane of a sheet, see Figure 6.

By quantum chemical calculations on the products of hydrogen desorption MgH_2, Al, and H_2, the hydrogen desorption enthalpy (41 kJ/mol compound) as well as the formation enthalpy (-64.8 kJ/mol) were determined.

Acknowledgment. We want to thank O. M. Løvvik, University of Oslo, who confirmed the sheet structure by DFT calculations with periodic boundary conditions.

IC034160Y